Proceedings of the ASME 2017 Dynamic Systems and Control Conference
DSCC2017
October 11-13, 2017, Tysons, Virginia, USA

DSCC2017-5391

GEOMETRIC GAIT DESIGN FOR A STARFISH-INSPIRED ROBOT WITH CURVATURE-CONTROLLED SOFT ACTUATORS

William L. Scott
Department of Aerospace Engineering
University of Maryland
College Park, MD 20742
Email: wlscott@umd.edu

Derek A. Paley
Department of Aerospace Engineering,
Institute for Systems Research
University of Maryland
College Park, MD 20742
Email: dpaley@umd.edu

ABSTRACT

This paper presents a geometric gait design and optimization framework for an idealized model of a planar starfish-inspired robot with curvature-controlled soft actuator arms. We describe the range of motion for each arm under the assumption of constant curvature along the length. Two modes of attachment of the ends of the arms to the ground are considered: fixed in position and orientation, and fixed in position but free to rotate. For each mode, we derive mathematical expressions for the local connection relating controlled shape changes to the displacement of the robot's center. For the rotating case, we additionally model the individual arms as ideal elastica beams and design gaits based on expected buckling behavior for a special case of symmetric (mirrored) curvature inputs via numerical simulations.

1 Introduction

The development of novel soft actuators that may combine bending, twisting, and lengthening action presents new opportunities in robot design [1]. The animal world provides many examples of organisms that achieve locomotion through periodic motion of soft appendages, and much recent work has focused on developing robot designs that mimic the body plan and locomotory capabilities of marine invertebrates. Starfish-inspired robots have been created using shape-memory alloy actuators [2], as well as designs driven by traditional motors with multiple rigid segments [3] and with passive compliant arms [4]. More recently an octopus robot was developed using entirely soft components, powered by chemical reactions and controlled by microfluidic oscillator circuits [5].

Robot architectures based on soft actuators with many underactuated degrees of freedom bring with them new challenges in mathematical modeling and control design. Methods from geometric control theory have been proposed as a means to accommodate nonlinear locomotive systems with many degrees of freedom [6]. A key concept in geometric control is the *local connection*, a mathematical operator that maps changes in the shape of a robot to its overall motion relative to the ground. In highly underactuated systems such as a flexible snake robot moving on sand it is possible to design efficient gaits by estimating the local connection experimentally [7].

Starfish, or sea stars, of class Asteroidea, along with the related brittle stars of class Ophiuroidea [8] serve as interesting model systems for control design due to the modularity inherent in their radial symmetry. In brittle stars it has been observed that different arms take on a leading role as the direction of motion changes [9]. A decentralized controller based on coupled oscillators was developed to achieve similar behavior in a brittle-star-inspired robot [4].

This paper presents an idealized model for a planar starfish-inspired robot with soft actuator arms. The robot is configured with a number of actuator arms mounted radially about a central hub. Each arm has constant length but variable controlled curvature, along with an anchor mechanism at the tip which can be activated to provide attachment to the ground surface. A design for retractable magnetic foot anchors has been developed [10]

that allows the robot to attach to a metal surface, e.g., the hull of a ship, in order to explore or perform inspections.

We consider arm actuators based on the "pneu-net" design [11] of a flexible rod with a network of internal air chambers that transforms pneumatic air pressure inputs into pure bending motion. This type of actuator can also be operated hydraulically with water as the operating fluid, and has been utilized underwater for grasping delicate sea creatures [12].

The relationship between input pressure and curvature along the length of a pneu-net actuator under end loading is studied in [13] using an elastica rod model. The elastica is a simple model for planar flexible rods with large deformations, such that the deviation in curvature at each point along the rod is proportional to the internal moment at that point. Equilibrium states for the elastica model are well studied, dating back to the work of Euler in the 18th century. Recent work on stability of equilibria for elastica rods based on strain-energy minimizing variational methods includes [14] and [15]. For our model, we first consider the arms to be rigid, allowing us to obtain exact analytic expressions for the movement of the center of the robot as a function of the input arm curvatures. Later when flexibility is added via an elastica model, we use numerical methods to estimate the connection between shape change and overall motion.

The contributions of this paper are (1) a framework for gait design and optimization for a novel soft-legged robot; (2) constraints on gait parameters (curvature control inputs) to achieve purely translational gaits; (3) categorizing gaits into classes based on symmetries of the starfish robot; (4) numerical results for classes of gait with optimal displacement or efficiency; and (5) illustrating how buckling of flexible actuators may be leveraged in gait design.

We introduce the mathematical model for the motion of the robot arms in Section 2. Section 3 considers the design of gaits for fixed foot connections. We derive conditions on gait parameters to enforce parallel motion and solve numerically for optimal gaits in that class. Section 4 discusses gaits for the case of rotating feet. We consider a modified model with flexible elastica arms in Section 5 and offer final remarks in Section 6.

2 Mathematical model

Consider a robot consisting of n identical soft actuator arms rigidly connected at a central point, arranged with radial symmetry. Arms are indexed as 0 through $n-1$ counterclockwise about the center. Let l be the constant length of each arm, and let $\beta = 2\pi/n$ be the angle separating each arm at the center. The robot moves on the plane, with position of its center $\mathbf{r}_c = (x_c, y_c)^T \in \mathbb{R}^2$, and orientation $\theta_c \in \mathbb{S}$ relative to the inertial frame with origin O. θ_c is measured counterclockwise from the x-axis to the tangent of arm 0 at the robot's center, as illustrated in Fig. 1.

Suppose that at the end of each arm, there is a foot

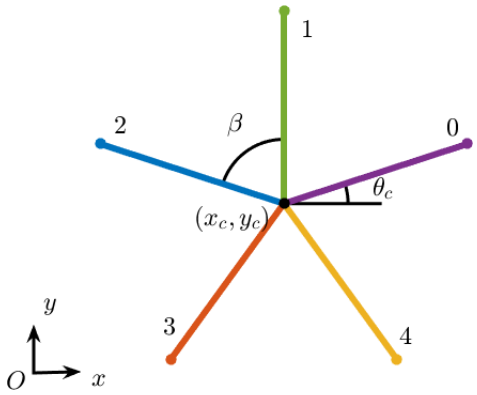

FIGURE 1. The 5-arm starfish robot with $\kappa_i = 0$ for all i.

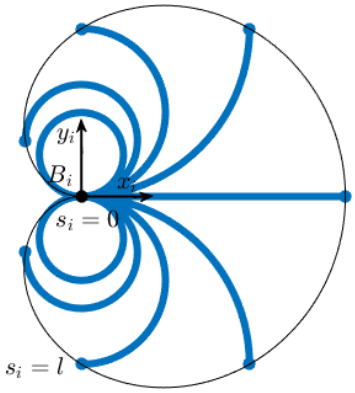

FIGURE 2. Range of motion of a single arm, with input curvature $\kappa_i = m\pi/(2l)$ for $m = \{-4, -3, ..., 4\}$

mechanism that can be activated to achieve contact with the ground/substrate. We consider two possible contact modes: *fixed* feet have a rigid contact that constrains the position and orientation of the foot; *rotating* feet constrain only the position, allowing the arm to rotate freely about the foot as in a pin joint.

Let the curvatures κ_i, $i = 0, ..., n-1$, be the control inputs, with $\kappa_i > 0$ and $\kappa_i < 0$ corresponding to counterclockwise and clockwise displacement of the arm with respect to the robot's center, respectively. Let $\bar{\kappa}$ be the maximum curvature for each arm.

The full state of the system can be partitioned into the $SE(2)$ *group variables* $\mathbf{r}_c = (x_c, y_c)^T \in \mathbb{R}^2$ and $\theta_c \in \mathbb{S}$ corresponding to the position of the center of the robot and its orientation on the plane, and the *shape variables* $\kappa = (\kappa_0, ... \kappa_{n-1})^T \in \mathbb{R}^n$ corresponding to the individual arm curvatures under the constraints $|\kappa_i| \leq \bar{\kappa}$ for $i = 0, ..., n-1$. A robotic gait refers to a periodic trajectory in the shape variables that gives rise to a net displacement in the group variables.

We consider the state of the system to vary quasistatically

with slow input changes. Thus the configuration at any moment in time is in an equilibrium state.

Fix a reference frame B_i onto the robot with the origin at the robot's center, and with its x-axis running along the length of a given arm i when it is fully extended with $\kappa_i = 0$. With the foot end free, i.e., with no applied forces, consider the motion of arm i as if it were rigid with constant curvature along its length. The arm forms a circular arc with radius $1/\kappa_i$. Parameterize material points along the arm by arc-length s_i measured from the center, out to $s_i = l$ at the foot. Let $\mathbf{a}(s_i, \kappa_i)$ be the displacement of the material point on arm i at arc length s_i from the center under curvature κ_i within the local frame for that arm, i.e.,

$$\mathbf{a}(s_i, \kappa_i) = \begin{cases} \frac{1}{\kappa_i}\begin{pmatrix} \sin(\kappa_i s_i) \\ 1-\cos(\kappa_i s_i) \end{pmatrix}, & \kappa_i \neq 0, \\ \begin{pmatrix} s_i \\ 0 \end{pmatrix}, & \kappa_i = 0. \end{cases}$$

For convenience, let $\mathbf{a}_l(\kappa_i) = \mathbf{a}(l, \kappa_i)$ refer to the position of foot i in frame B_i. For $\kappa_i = 2\pi/l$, the arm forms a full circle, with the foot at the base of the arm. The tangent vector along the arm is given by $\mathbf{a}'(s_i, \kappa_i) = \frac{\partial}{\partial s_i}\mathbf{a}(s_i, \kappa_i) = (\cos(\kappa_i s_i), \sin(\kappa_i s_i))^T$. The orientation of the foot in frame B_i is $\theta_i(l) = l\kappa_i$.

In the inertial reference frame, the location of foot i is

$$\mathbf{p}_i = \mathbf{r}_c + R(\theta_c + \beta i)\mathbf{a}_l(\kappa_i), \tag{1}$$

where R is the standard rotation matrix in $SO(2)$, and the orientation of foot i is

$$\phi_i = \theta_c + \beta i + l\kappa_i. \tag{2}$$

3 Gait design for fixed-orientation anchors

This section defines a framework to parameterize gaits for a robot with feet that can be anchored to the ground with fixed position and fixed orientation. Suppose that only one anchor is active at any given time, with instantaneous switches between active arms at discrete times. In the case of fixed attachment, the motion of the center of the robot is completely constrained by the motion of the active arm. The curvatures of the inactive arms do not contribute at all to the motion, and may be ignored until such time that a new arm becomes active.

Definition: Gait $G = \{S_m\}$, $m = 1, ..., M$ is defined as a set of one or more steps, $S_m = (\kappa^{m-}, \kappa^{m+}, \Delta_m)$, with each step S_m defined by three parameters: the beginning and ending curvatures for the active (anchored) arm, $\kappa^{m-}, \kappa^{m+} \in \mathbb{R}$, and the index offset Δ_m that specifies the next active arm. A single gait cycle is a trajectory comprising steps S_1 through S_M in succession.

Consider a gait with a single step $G = \{(a, b, c)\}$, and suppose, at the start of the step, arm i activates with initial curvature $\kappa_i = a$. Arm i bends to curvature value $\kappa_i = b$, which causes the center of the robot to move relative to the anchored foot. Once arm i reaches the desired curvature, arm $j = (i + c) \bmod n$ brings its own curvature to $\kappa_j = a$ and becomes active, anchoring its foot and restarting the process for the next step. (To increase speed, the next arm may begin moving toward its desired curvature κ^- before the active arm reaches κ^+, but this will not affect the displacement for the step.)

We derive the displacement of the group variables for a single step S_m as a function of the step parameters by setting the location and orientation of the anchored foot at the initial and final configurations to be equal. Let the initial state at time t^- be described by $\mathbf{r}_c^-$, θ_c^-, with curvature $\kappa_i(t^-) = \kappa^{m-}$ in the active arm i, and similarly for the final state at time t^+, $\mathbf{r}_c^+$, θ_c^+, with active arm curvature $\kappa_i(t^+) = \kappa^{m+}$. We solve for the displacements $\Delta\theta_c^m = \theta_c^+ - \theta_c^-$ and $\Delta\mathbf{r}_c^m = \mathbf{r}_c^+ - \mathbf{r}_c^-$ via (1) and (2):

$$\begin{aligned} \phi_i(t^-) &= \phi_i(t^+), \\ \theta_c^- + \beta i + l\kappa^{m-} &= \theta_c^+ + \beta i + l\kappa^{m+}, \\ \Delta\theta_c^m = \theta_c^+ - \theta_c^- &= l(\kappa^{m-} - \kappa^{m+}), \end{aligned}$$

which implies

$$\begin{aligned} \mathbf{p}_i(t^-) &= \mathbf{p}_i(t^+), \\ \mathbf{r}_c^- + R(\theta_c^- + \beta i)\mathbf{a}_l(\kappa^{m-}) &= \mathbf{r}_c^+ + R(\theta_c^+ + \beta i)\mathbf{a}_l(\kappa^{m+}), \\ \Delta\mathbf{r}_c^m = \mathbf{r}_c^+ - \mathbf{r}_c^- &= R(\phi_i - l\kappa^{m-})\mathbf{a}_l(\kappa^{m-}) - R(\phi_i - l\kappa^{m+})\mathbf{a}_l(\kappa^{m+}), \\ &= R(\phi_i)[\mathbf{a}_l(-\kappa^{m-}) - \mathbf{a}_l(-\kappa^{m+})]. \end{aligned} \tag{3}$$

Note that the direction of $\Delta\mathbf{r}_c^m$ depends on the orientation of the active foot, ϕ_i.

At the end of step S_m, arm $(i + \Delta_m) \bmod n$ activates the anchor at its foot. The difference in orientations for successive foot anchors determines whether a given gait follows a straight line or a curved trajectory over multiple gait cycles. Let $\Delta\phi^m$ be the difference in foot orientations from arm i to arm $j = (i + \Delta_m) \bmod n$ at the end of step S_m:

$$\begin{aligned} \Delta\phi^m &= \phi_j - \phi_i \\ &= (\theta_c(t) + \beta j + l\kappa_j(t)) - (\theta_c(t) + \beta i + l\kappa_i(t)), \\ &= \beta(j - i) + l(\kappa_j(t) - \kappa_i(t)) \\ &= \beta\Delta_m + l(\kappa^{(m+1)-} - \kappa^{m+}). \end{aligned} \tag{4}$$

Theorem 1. *If the steps in a gait satisfy the condition*

$$\cos\left(\sum_{m=1}^{M} \beta\Delta_m + l(\kappa^{m-} - \kappa^{m+})\right) = 1, \tag{5}$$

then the net displacement in position for each gait cycle will be parallel over repeated gait cycles.

Proof. We show that the condition (5) implies that the orientation of the active foot at the start of each cycle is the same, which further implies that the displacement vectors for subsequent cycles are parallel. Let $j(m)$ be the active arm for step m in the gait, such that $j(m+1) = (j(m)+\Delta_m) \bmod n$, with $j(1) = 0$. The difference in stance foot orientation from one gait cycle to the next, denoted $\Delta\phi^G$, is the sum of differences for each step in a gait cycle:

$$\Delta\phi^G = \sum_{m=1}^{M} \Delta\phi^m = \sum_{m=1}^{M} \beta\Delta_m + l(\kappa^{(m+1)-} - \kappa^{m+})$$

Since the steps in the next gait cycle are the same as the steps in this cycle, $\kappa^{(M+1)-} = \kappa^{1-}$. Also since we are summing over all steps, we can change the index in a term without changing the value of the sum, thus

$$\Delta\phi^G = \sum_{m=1}^{M} \beta\Delta_m + l(\kappa^{m-} - \kappa^{m+}).$$

The condition (5) constrains the net orientation change of the stance foot over the course of a gait cycle to be zero.

Having the same stance foot orientation at the start of successive gait cycles implies that the net motion is purely translational (up to a renaming of the identical arms). The displacement of the center for one gait cycle is given by the sum of displacements from (3), i.e.,

$$\Delta\mathbf{r}_c^G = \sum_{m=1}^{M} \Delta\mathbf{r}_c^m = \sum_{m=1}^{M} R(\phi_{j(m)})[\mathbf{a}_l(-\kappa^{m-}) - \mathbf{a}_l(-\kappa^{m+})].$$

Note that $\phi_{j(m)} = \phi_{j(1)} + \sum_{q=1}^{m-1}(\phi_{j(q+1)} - \phi_{j(q)}) = \phi_0 + \sum_{q=1}^{m-1}\Delta\phi^q$ from (4). Taking the convention that $\sum_{q=1}^{0}\Delta\phi^q = 0$ for the $m = 1$ term, we rewrite the sum to pull out the dependence on the initial foot orientation,

$$\begin{aligned}\Delta\mathbf{r}^G &= \sum_{m=1}^{M} R\left(\phi_0 + \sum_{q=1}^{m-1}\Delta\phi^q\right)[\mathbf{a}_l(-\kappa^{m-}) - \mathbf{a}_l(-\kappa^{m+})],\\ &= R(\phi_0)\sum_{m=1}^{M} R\left(\sum_{q=1}^{m-1}\Delta\phi^q\right)[\mathbf{a}_l(-\kappa^{m-}) - \mathbf{a}_l(-\kappa^{m+})].\end{aligned}$$

The cycle displacement vector is pre-multiplied by a rotation matrix corresponding to the initial stance foot orientation and is otherwise only a function of the gait parameters. From this observation, we see that the only way for successive cycles to yield parallel displacements is for the orientation of the initial stance foot to be the same at the start of each cycle, which is achieved when the condition (5) is satisfied. □

The following subsections categorize fixed-foot gaits into different types and analyze the performance.

3.1 Single-step gaits: rolling motion

For a robot with n arms, there are a family of single-step gaits $G_{\text{roll}} = \{(\kappa^{1-}, \kappa^{1+}, \Delta_1)\}$ that satisfy the parallel motion constraint (5) for each value of $\Delta_1 \in \{1, ..., n-1\}$. For a chosen value of Δ_1, the difference in curvature for the active arm is constrained to be $\kappa^* = \kappa^{1+} - \kappa^{1-} = 2\pi\Delta_1/n$ for clockwise rotation, with opposite sign for counterclockwise rotation. The family of gaits is characterized by a single parameter κ^0, with $\kappa^{1-} = \kappa^0 - \kappa^*/2$ and $\kappa^{1+} = \kappa^0 + \kappa^*/2$.

By choosing a suitable cost function, we can solve for the optimal value of κ^0 given the parameters of the system. Consider the following two objectives: maximum displacement per step, and maximum efficiency. Efficiency is defined as the displacement magnitude divided by a measure of the input control effort. We choose the L_1 norm of the input curvature rate on the anchored arm as a measure of the control effort:

$$\text{Effort} = \int_0^T |\dot{\kappa}_{\text{anchored}}| dt = \kappa^{1+} - \kappa^{1-},$$

which is independent of the time taken to move the arm from κ^{1-} to κ^{1+}. In order to satisfy the parallel motion constraint (5), the effort is determined by Δ_1. Thus within a Δ_1-rolling-gait family, the maximum-displacement gait is also the maximum-efficiency gait.

To find the value of κ^0 that yields the highest displacement magnitude, i.e.,

$$\begin{aligned}||\Delta\mathbf{r}^G(\kappa^0)|| &= ||\mathbf{a}_l(-\kappa^{1-}) - \mathbf{a}_l(-\kappa^{1+})||\\ &= ||\mathbf{a}_l(-\kappa^0 + \kappa^*/2) - \mathbf{a}_l(-\kappa^0 - \kappa^*/2)||,\end{aligned}$$

we take the derivative with respect to κ^0 and set it equal to zero. Note that $||\Delta\mathbf{r}^G(\kappa^0)||$ is even about $\kappa^0 = 0$, which is its global maximum for all Δ_1 families (calculated numerically). Figure 3 illustrates the displacement and efficiency for various numbers of arms n and values of Δ_1. For each number of arms, we find that the $\Delta_1 = 1$ gait yields the lowest displacement but the highest efficiency. This gait is illustrated in Fig. 4 for $n = 3$ arms.

3.2 Two-step gaits: walking motion

Gaits with two steps are defined by six parameters, $G = \{(\kappa^{a-}, \kappa^{a+}, \Delta_a), (\kappa^{b-}, \kappa^{b+}, \Delta_b)\}$. Two gaits with the same steps in a different order are equivalent. Swapping κ^+ with κ^- and

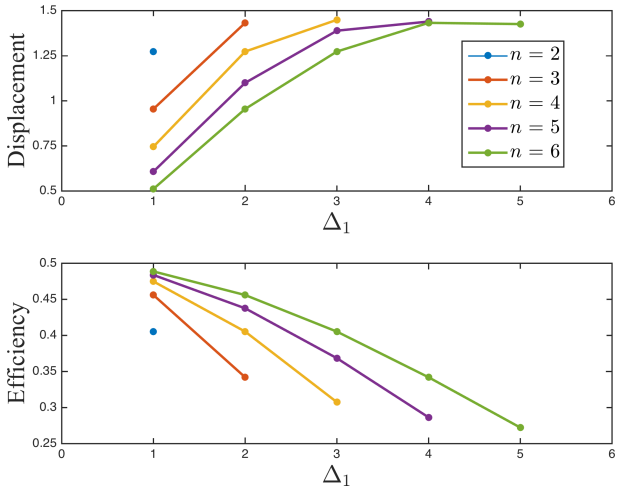

FIGURE 3. Maximum center displacement magnitude and efficiency per step for rolling gaits with fixed foot anchors as a function of Δ_1 for varying number of arms n. For any number of arms, $\Delta_1 = 1$ yields the lowest displacement but highest efficiency.

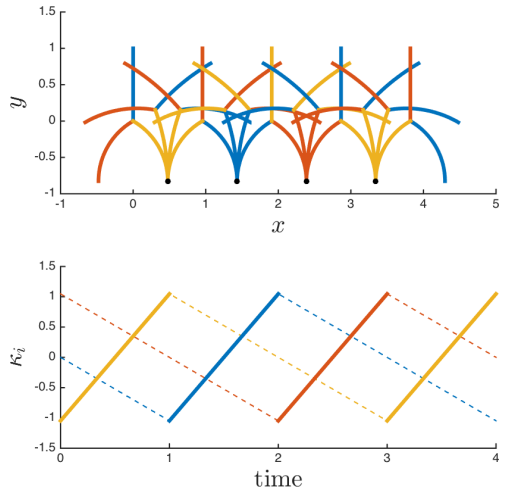

FIGURE 4. Illustration of the maximum efficiency rolling gait for $n = 3$ arms, $G = \{(-\pi/3, \pi/3, 1)\}$. Upper plot shows snapshots of the robot state in inertial coordinates at time intervals of $1/3$ second, with anchored foot shown as a black dot. Lower plot shows trajectories of the shape variables over time, with solid line for active (anchored) arm.

changing the sign of Δ within each step yields a gait with per cycle displacement of the same magnitude as the original, but in the opposite direction.

We define a symmetric walking gait as a two-step gait with alternating arms, such that $\Delta_b = -\Delta_a$. We find through numerical optimization that for symmetric walking gaits satisfying the parallel motion constraint (5), the highest per cycle displacement is

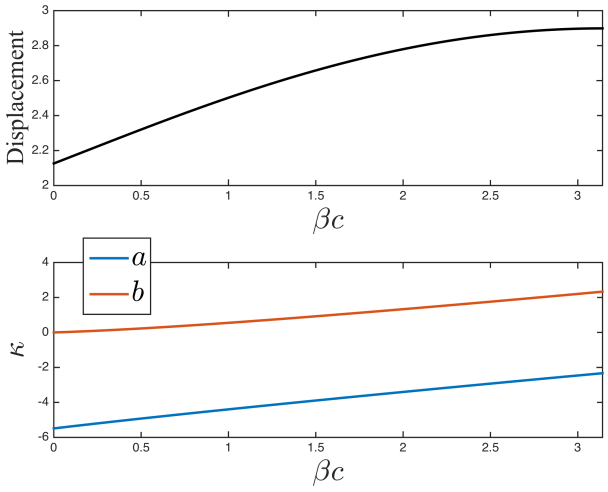

FIGURE 5. Maximum per cycle displacement magnitudes and the associated optimal gait parameters a and b as a function of βc for alternating-arm walking gaits with fixed foot anchors in the form $G = \{(a,b,c),(-a,-b,-c)\}$. Maximum per cycle displacement magnitude is achieved when $\beta c = \pi$, as in a two arm robot, with $b = -a \approx 2.331$.

achieved by gaits in the form $G = \{(a,b,c),(-a,-b,-c)\}$. Figure 5 shows the optimal values of the a and b curvature parameters as the value of βc (the offset angle between the alternating arms) is varied.

In two-step gaits, if we instead optimize for maximum efficiency as defined above, the optimal gaits have infinitesimal changes in curvature for each step. This outcome is related to the observation above that efficiency rises as the number of arms increases, with each individual step having decreasing displacement. In reality, there will be some cost associated with the activation and deactivation of the anchors at the feet. By adding a constant value to the denominator of the efficiency calculation, we recover feasible optimal gaits, with the optimal gait approaching the maximum displacement gait as the switching cost approaches infinity.

4 Gait design for rotating anchors

Now consider gaits for a robot with feet that can rotate about their anchor point. With rotating anchors, two arms must have their feet anchored at any given time in order to control the motion of the system. Otherwise with only one anchor point, the whole robot might rotate freely about the single anchor. By convention, label the two anchored arms as arm i and arm j, with angular offset of β.

Once two arms are anchored, the feet are separated by a constant distance d. To achieve motion, the curvature change in the two arms must be coordinated such that the constant foot distance constraint is not violated. The foot distance d as a function

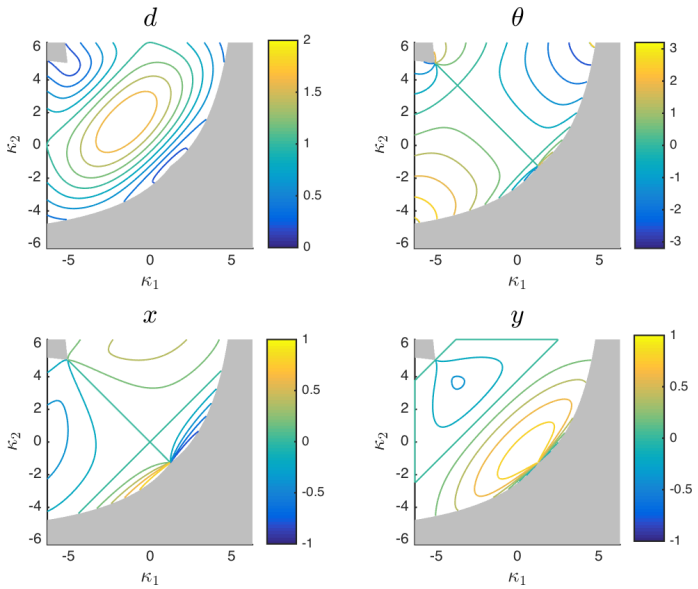

FIGURE 6. Top left: Distance from foot 1 to foot 2 as a function of the arm curvatures κ_1 and κ_2, based on inter-arm angle $\beta = 2\pi/5$ with unit arm length $l = 1$. Configurations where the two stance arms cross are shaded. Contours drawn at intervals of 0.2. For rotating feet, the trajectory in stance phase must travel along a contour of constant d. The remaining three plots show the relative position and orientation of the center in the stance frame as a function of the input curvatures. For θ, contours are drawn at intervals of $\pi/5$ radians. For x and y, contours are drawn at intervals of 0.2.

of curvature inputs is

$$d = ||\mathbf{p}_i - \mathbf{p}_j|| = ||\mathbf{a}_l(\kappa_i) - R(\beta)\mathbf{a}_l(\kappa_j)|| = \text{constant}.$$

Thus, during a stance phase, the motion of the arms is constrained to satisfy

$$\dot{d} = \frac{\partial d}{\partial \kappa_i}\dot{\kappa}_i + \frac{\partial d}{\partial \kappa_j}\dot{\kappa}_j = 0.$$

The gait design for rotating feet is equivalent to the design for fixed feet, except that now instead of considering motion relative to an inertial frame fixed at a single foot we use a stance frame B_{ij} defined by the position of the two anchored feet i and j. Let the origin of B_{ij} be located at the midpoint between the feet, $(\mathbf{p}_i + \mathbf{p}_j)/2$, oriented such that its x-axis is in the direction of the baseline vector from foot i to foot j, $\mathbf{p}_j - \mathbf{p}_i$. For gait design, consider the translation and rotation of the robot center in this frame, measuring θ_c as it deviates from its orientation at a reference configuration with $\kappa_j = -\kappa_i$. Figure 6 shows how

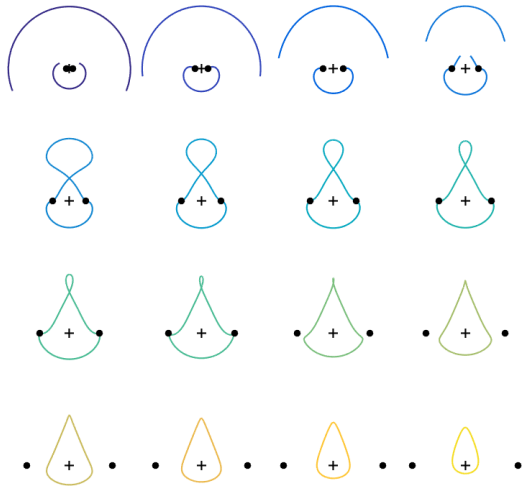

FIGURE 7. Admissible center trajectories for rotating feet with various foot distances. Foot distance d increases across rows from top to bottom, with $d = 0.1l, 0.2l, ..., 1.6l$. Origin of the stance frame is denoted with $+$, and dots show the foot locations. All plots use $\beta = 2\pi/5$, corresponding to the 5-armed robot with neighboring arms anchored.

the group variables in the stance frame vary as a function of the arm curvatures, and Fig. 7 illustrates the trajectories of the robot center for arm curvatures following selected constant-d contours. Configurations where the two arms cross each other are omitted.

While there is still a single degree of freedom for body motion within a single stance phase, we have the additional parameter of the foot distance to allow for a wider variety of possible gaits. The gait description for rotating feet requires six parameters for each step: $S_m = ({}^a\kappa^{m-}, {}^a\kappa^{m+}, {}^b\kappa^{m-}, {}^b\kappa^{m+}, {}^{ab}\Delta_m, \Delta_m)$, where ${}^a\kappa^{m-}$, ${}^a\kappa^{m+}$, ${}^b\kappa^{m-}$, and ${}^b\kappa^{m+}$ refer to the starting and ending curvatures of the two active arms, $i_a(m)$ and $i_b(m)$, respectively. ${}^{ab}\Delta_m$ is the index offset between the stance arms, such that $i_b(m) = (i_a(m) + {}^{ab}\Delta_m) \bmod n$, and Δ_m is the index offset for the next step, such that $i_a(m+1) = (i_a(m) + \Delta_m) \bmod n$.

As an analog to the symmetric rolling gaits for fixed foot anchors, we seek single step gaits where the orientation of successive stance frames are the same. In the case of a robot with $n = 5$ arms, we consider gaits of the form $G = \{(c_1, c_2, -c_2, -c_1, 1, 2)\}$. The parallel motion condition is satisfied here if the angle of the center in the stance frame satisfies $\theta_c = \pm\beta$ at the beginning of the stance phase, with clockwise rolling for positive and counterclockwise for negative. One such gait is illustrated in Fig. 8 for $n = 5$ with $c_1 \approx 2.201$ and $c_2 \approx 0.3625$. These parameters were numerically optimized to achieve the maximum per step displacement while satisfying the parallel motion condition and avoiding arm crossings.

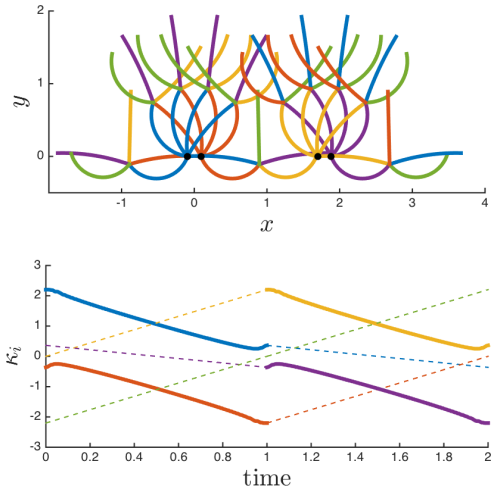

FIGURE 8. Illustration of a rolling gait for $n = 5$ arms with rotating feet. Upper plot shows snapshots of the robot state in inertial coordinates at time intervals of $1/5$ second, with anchored foot shown as a black dot. Lower plot shows trajectories of the shape variables over time, with solid lines for active (anchored) arms.

5 Adding flexibility: elastica arm model

Thus far in our analysis we have treated our soft actuators as though they were rigid, with arm curvature directly and exactly controlled by the user. This assumption simplifies the geometry and limits the parameter space for gait design at the cost of removing some degrees of freedom. In reality, a soft robot is an underactuated system with infinite degrees of freedom associated with the deformed state of the compliant structures.

The following analysis reintroduces the flexibility of the actuators into the system by modeling each arm as an idealized elastica beam with its intrinsic curvature determined by the control input, free to deform under the forces due to the boundary conditions at the foot anchors.

5.1 Static equilibria for two elastica arms anchored with rotating feet

Suppose arms i and j with offset angle β have their feet anchored via rotating pin joint at points $\mathbf{p}_i$, $\mathbf{p}_j$ a distance d apart. As before, let B_{ij} be a frame aligned with the baseline vector from foot i to foot j with its origin at the midpoint between the feet. For each arm, let s_i be the arc length of the arm measured starting from the foot with $s_i = 0$, ending at the robot center at $s_i = l$.

The bending stress in the arms will cause some forces $\mathbf{F}_i = F\mathbf{e}_x$, $\mathbf{F}_j = -F\mathbf{e}_x$ at the feet with unknown magnitude F, aligned with the baseline between the feet. The arm angles at the feet $\theta_i(0)$ and $\theta_j(0)$ are also unknown. At the robot center point where the arms meet, the difference between the angles is $\theta_j(l) - \theta_i(l) = \beta$. The rotating anchor at the foot does not apply an external moment, so the curvature boundary conditions are $\theta_i'(0) = l\kappa_i$ and $\theta_j'(0) = l\kappa_j$.

The constraints ensuring that the arms meet at the center of the body are

$$\int_0^l \cos(\theta_i(s))\mathrm{d}s - \int_0^l \cos(\theta_j(s))\mathrm{d}s = d, \text{ and}$$
$$\int_0^l \sin(\theta_i(s))\mathrm{d}s - \int_0^l \sin(\theta_j(s))\mathrm{d}s = 0.$$

Or, equivalently, since $x_i'(s) = \cos(\theta_i(s))$ and $y_i'(s) = \sin(\theta_i(s))$ in frame B_{ij}, the constraints can be written as $x_1(l) - x_2(l) = d$ and $y_1(l) = y_2(l)$.

The total potential energy for arm i is [15]

$$\Pi_i = \int_0^l \tfrac{1}{2} EI(\theta_i'(s) - \kappa_i)^2 \mathrm{d}s,$$

for flexural rigidity EI and nominal (input) curvature κ_i, which here is assumed constant along the length of the arm for ease of analysis. In general, a pneu-net soft actuator will have varying intrinsic curvature along its length, with lower curvature towards the ends (shown experimentally in [13]). Applying the unknown force $\mathbf{F}_i$ as a Lagrange multiplier, the energy functional has extrema at solutions of the Euler-Lagrange equation [15]

$$\theta_i'' = \frac{F}{EI}\sin(\theta_i), \tag{6}$$

which satisfy the boundary constraints, corresponding to equilibrium solutions for the shape of the arm.

Note that in general multiple solutions exist with different forces and foot angles.

5.2 Predicted buckling behavior of rotating foot system with symmetric inputs

Consider the symmetric case for two arms where $\kappa_j = -\kappa_i$. For a range of foot distances d there are some curvature values that accommodate multiple equilibrium configurations, which give rise to buckling instabilities and hysteresis as the curvature is varied.

If we limit our investigation to only symmetric configurations ($x_c = 0, \theta_c = 0$), we can analyze a single arm by considering the base of the arm as fixed and allowing the foot to rotate and translate along the y_c-axis in frame B_{ij}. A similar problem was investigated in [16, 17] for curved beams in the case that $\beta = \pi$ with freely rotating ends and translating end under a constant load at the free end, and in [18] for straight rods with fixed ends.

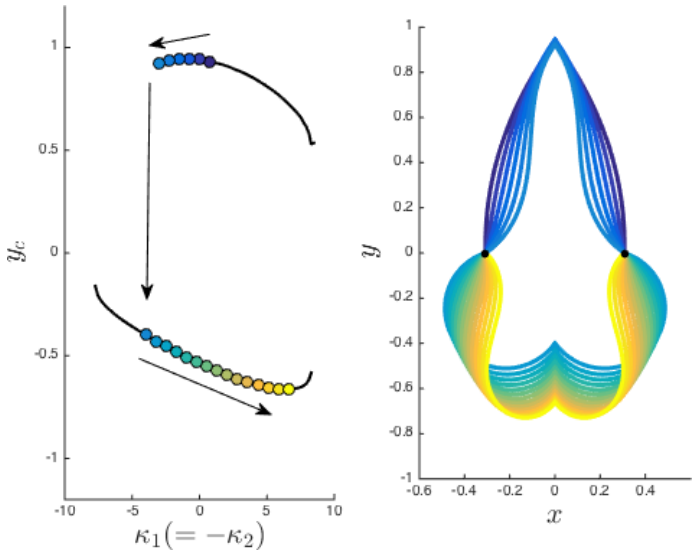

FIGURE 9. Buckling trajectory for symmetric elastica arms with rotating feet, for $l = 1$, $d \approx 0.613$, $\beta = 2\pi/5$. Left: Height of the robot center y_c vs. the input curvature κ_1. Starting on the upper branch, κ_1 decreases until no stable equilibrium exists, whereupon buckling occurs and the state jumps an equilibrium configuration on the lower branch. κ_1 is then increased to further lower the center for maximum displacement. Right: Shapes of the elastica arms at snapshots through the trajectory, with colors matching the points on the figure on the left.

For a given value of d, there are typically two values of κ_i that yield an equilibrium with zero forces acting at the feet (the geometrically constrained configurations considered in Section 4). We numerically solve the boundary value problem for the foot force F and foot angle $\theta_i(0)$ by slowly varying κ_i in either direction from the zero-force solutions. The Matlab numerical optimization function *fminunc* was used to solve for $\theta_i(0)$ and F corresponding to arm shapes that satisfy the boundary conditions for the symmetric elastica with $\kappa_j = -\kappa_i$. Using cost function $J = (x_i(l) - d/2)^2 + (1 - \cos(\theta_i(l) - (pi/2 - \beta/2)))^2$, the boundary conditions $x_i(l) = d/2$ and $\theta_i(l) = \pi/2 - \beta/2$ are satisfied when $J = 0$.

Figure 9 illustrates a proposed symmetric trajectory that maximizes the displacement in the y_c direction for a given foot distance. Starting at the $F = 0$ configuration on the upper branch, the curvature is varied until no equilibrium solution satisfying the boundary conditions is found. We predict that at that point the arms buckle, bringing the system to an equilibrium on the lower branch. Work is ongoing to rigorously characterize the stability of the numerical solutions.

6 Conclusion

We present a mathematical model for locomotion in a starfish-inspired robot with curvature-controlled soft actuators. For both fixed and rotating modes of foot anchor attachment, we develop a framework for describing periodic gaits and derive conditions on gait parameters to ensure travel in a straight line across multiple gait cycles. For the rotating case, we additionally model the individual arms as ideal elastica beams, finding examples of bistability and hysteresis in numerical simulations that may be useful in gait design.

In ongoing work, we aim to characterize the entire space of equilibria for the flexible elastica arms and estimate the local connection in order to optimize gaits as in [7]. Experiments on a physical prototype robot will enable us to refine our model and optimize gaits further.

ACKNOWLEDGMENT

We thank Michael Bell, Kaitlyn Becker, and Robert Wood at Harvard University for inspiration and helpful discussions. This work was funded in part by ONR Grant N000141712063.

REFERENCES

[1] Marchese, A. D., Katzschmann, R. K., and Rus, D., 2015. "A recipe for soft fluidic elastomer robots". *Soft Robotics,* ***2***(1), pp. 7–25.

[2] Mao, S., Dong, E., Jin, H., Xu, M., Zhang, S., Yang, J., and Low, K. H., 2014. "Gait study and pattern generation of a starfish-like soft robot with flexible rays actuated by SMAs". *J. Bionic Engineering,* ***11***(3), pp. 400–411.

[3] Lal, S. P., Yamada, K., and Endo, S., 2008. "Evolving motion control for a modular robot". In *Applications and Innovations in Intelligent Systems XV*. Springer, pp. 245–258.

[4] Watanabe, W., Suzuki, S., Kano, T., and Ishiguro, A., 2011. "Moving right arm in the right place: Ophiuroid-inspired omnidirectional robot driven by coupled dynamical systems". In Proc. IEEE/RSJ Int. Conf. on Intelligent Robots and Systems, pp. 1895–1900.

[5] Wehner, M., Truby, R. L., Fitzgerald, D. J., Mosadegh, B., Whitesides, G. M., Lewis, J. A., and Wood, R. J., 2016. "An integrated design and fabrication strategy for entirely soft, autonomous robots". *Nature,* ***536***(7617), pp. 451–455.

[6] Aguilar, J., Zhang, T., Qian, F., Kingsbury, M., McInroe, B., Mazouchova, N., Li, C., Maladen, R., Gong, C., Travers, M., et al., 2016. "A review on locomotion robophysics: the study of movement at the intersection of robotics, soft matter and dynamical systems". *Reports on Progress in Physics,* ***79***(11), p. 110001.

[7] Dai, J., Faraji, H., Gong, C., Hatton, R. L., Goldman, D. I., and Choset, H., 2016. "Geometric swimming on a granular surface". In Proc. Robotics: Science and Systems.

[8] Lawrence, J. M., 1987. *A functional biology of echinoderms*. Croon Helm, London.

[9] Astley, H. C., 2012. "Getting around when you're round: quantitative analysis of the locomotion of the blunt-spined brittle star, *Ophiocoma echinata*". *J. Experimental Biology,* ***215***(11), pp. 1923–1929.

[10] Bell, M., Becker, K. P., and Wood, R. J., 2017. Personal communication.

[11] Mosadegh, B., Polygerinos, P., Keplinger, C., Wennstedt, S., Shepherd, R. F., Gupta, U., Shim, J., Bertoldi, K., Walsh, C. J., and Whitesides, G. M., 2014. "Pneumatic networks for soft robotics that actuate rapidly". *Advanced Functional Materials,* ***24***(15), pp. 2163–2170.

[12] Galloway, K. C., Becker, K. P., Phillips, B., Kirby, J., Licht, S., Tchernov, D., Wood, R. J., and Gruber, D. F., 2016. "Soft robotic grippers for biological sampling on deep reefs". *Soft Robotics,* ***3***(1), pp. 23–33.

[13] de Payrebrune, K. M., and O'Reilly, O. M., 2016. "On constitutive relations for a rod-based model of a pneu-net bending actuator". *Extreme Mechanics Letters,* ***8***, pp. 38–46.

[14] O'Reilly, O. M., and Peters, D. M., 2011. "On stability analyses of three classical buckling problems for the elastic strut". *J. Elasticity,* ***105***(1), pp. 117–136.

[15] Levyakov, S. V., and Kuznetsov, V. V., 2010. "Stability analysis of planar equilibrium configurations of elastic rods subjected to end loads". *Acta Mechanica,* ***211***(1), pp. 73–87.

[16] Hymans, F., 1946. "Flat spring with large deflections". *Trans. ASME, J. Applied Mechanics,* ***13***(68), pp. A223–A230.

[17] De Bona, F., and Zelenika, S., 1997. "A generalized elastica-type approach to the analysis of large displacements of spring-strips". *Proc. IMechE Part C, J. Mechanical Engineering Science,* ***211***(7), July, pp. 509–517.

[18] Thacker, W. I., Wang, C. Y., and Watson, L. T., 2008. "Effect of flexible joints on the stability and large deflections of a triangular frame". *Acta Mechanica,* ***200***(1), pp. 11–24.